Total (elastic plus inelastic) cross sections for electron scattering from diatomic and polyatomic molecules at 10–5000 eV: H_2, Li_2, HF, CH_4, N_2, CO, C_2H_2, HCN, O_2, HCl, H_2S, PH_3, SiH_4, and CO_2

Ashok Jain and K. L. Baluja*
Physics Department, Florida A&M University, Tallahassee, Florida 32307
(Received 23 May 1991; revised manuscript received 28 August 1991)

By employing a previously proposed model [A. Jain, Phys. Rev. A **34**, 3703 (1986); J. Phys. B **22**, 905 (1988)], we report calculations on the total (elastic plus inelastic) electron-scattering cross sections in a wide energy range (10–5000 eV) from several diatomic and polyatomic molecular targets (H_2 Li_2, HF, CH_4, N_2, CO, C_2H_2, HCN, O_2, HCl, H_2S, PH_3, SiH_4, and CO_2). A model complex optical potential (composed of static, exchange, polarization, and absorption terms) is calculated for each collision system from the corresponding molecular wave function at the Hartree-Fock level. The resulting complex optical potential, free from any adjustable parameter, is treated exactly in a variable-phase approach to yield scattering complex phase shifts and the total cross sections. In the intermediate- and high-energy region, the small contribution due to the nonspherical nature of the target is treated perturbatively in the first-order Born approximation. The present method is quite simple in nature and is able to reproduce fairly well the experimental total cross sections in the present energy region. Results are also given for individual elastic and absorption (accounting for all energetically possible inelastic processes in an approximate way) cross sections. In addition, we provide Born-Bethe parameters for all the above molecules including those of H_2O and NH_3. We have also examined the correlation between molecular properties and the total-cross-section parameter. For molecules possessing a permanent dipole or quadrupole moment, the present results are only roughly reliable above 100 eV.

PACS number(s): 34.80.−i, 34.90.+q, 52.20.Fs, 61.80.Fe

I. INTRODUCTION

The total cross sections (σ_t) (including elastic plus all energetically possible inelastic channels) for electron-molecule systems are important in many applied sciences [1–5]. Here we are interested in the intermediate- and high-energy region (roughly from ionization threshold up to several keV), where almost all inelastic channels (rotational, vibrational, and electronic excitation, ionization, dissociative processes, etc.) are open. In this energy regime, a conventional close-coupling theory [6–9] of the electron-molecule complex is an arduous task and almost impossible to carry out with present-day fast supercomputers. It is, therefore, not surprising that almost all previous calculations on the σ_t for electron-molecule systems have been restricted to a low-energy region (typically below or around the first ionization threshold) only. Several review articles, both experimental and theoretical, have recently described the progress made in the area of electron-molecule collisions in general (see Ref. [8]). Although it is in the low-energy electron-molecule scattering where the cross sections exhibit a rich structure and several complex phenomena [6–9], a knowledge of high-energy σ_t values for several molecular gases is required [1–5]. The importance of σ_t in radiation physics and chemistry has been discussed in the literature [10]. Such cross sections are available mostly through experimental studies, and theoretical σ_t values in the literature are scarce (see Table I), even for the simplest H_2 molecule.

The intermediate- and high-energy electron-impact calculations on the total cross sections for several molecular targets (CH_4, SiH_4, H_2O, and NH_3) are available to date due to one of the present authors [11,12], who employed a simple approach based on the spherical-complex-optical potential (SCOP) of the given electron-target system. Some semiempirical calculations were carried out on the σ_t e-H_2 scattering by van Wingerden, Wagenaar, and de Heer [13] at 20–2000 eV. Staszewska, Schwenka, and Truhlar [14] have employed a close-coupling complex-optical-potential approach to study e-H_2 elastic, absorption, and total cross sections at 10, 40, and 100 eV only. Recently, Itikawa *et al.* [15] have compiled e-N_2 total cross sections in the range of 0–200 eV. The other theoretical results on the e-H_2, N_2, and O_2 intermediate- and high-energy σ_t cross sections were published by Liu [16], who used a Born-Bethe-type theory [17–24], which gives good results on the total cross sections at very high energies, particularly in the keV region. However, the availability of Born-Bethe parameters in the literature for molecules studied in this paper is not satisfactory. In addition, the energy range of a few hundred eV to a few keV, where most of the experimental σ_t values are obtained, may not be suitable for such Born-type calculations [16].

In the SCOP method, the spherical part of the complex optical potential is treated exactly in a partial-wave analysis to yield cross-section parameters. The neglect of nonspherical terms in the full expansion of the optical potential is based on the fact that such an anisotropic con-

TABLE I. Summary of total cross sections (σ_t) available in the literature for electron scattering with various molecules studied in this work. Note that the low-energy (below 10 eV) references are excluded from the table.

Molecule	Expt. (energy range in eV) reference	Previous calculations
H_2	(25–750) [13]; (0.02–100) [38]; (2–500) [41] (8–400) [42]; (20–2000) [13]	(100–2000) [16]; (20–2000) [13] (10–100) [14]
Li_2	(0.5–10) [44]	(0–10) [95]
HF	None	(0–20) [96]
CH_4	(1–500) [57]; (1.3–50) [63]; (5–400) [64] (1–400) [66]; (0.1–20) [67]; (1–500) [68]; (75–4000) [69]	(0.1–500) [11]
NH_3	(1–400) [25]; (1–80) [26]	(10–3000) [12]
H_2O	(81–3000) [29]; (0.5–80) [30] (1–400) [31]; (7–500) [32]; (25–300) [33]	(10–3000) [12]
N_2	(7–500) [32]; (2.2–700) [41]; (1.2–403) [48]	(100–2000) [16]
CO	(1–500) [47]; (1.2–403) [48]; (380–5200) [49] (600–5000) [53]; (100–1600) [52]; (15–750) [51]	
C_2H_2	(1–400) [61]	None
HCN	None	(0–20) [96]
O_2	(100–1600) [52]; (0.5–25) [54]; (0.8–50) [55]; (0.2–100) [56] (1–500) [57]	(100–2000) [16]
HCl	(1–400) [59]	None
SiH_4	(1–400) [71]	(10–500) [11]
PH_3	None	None
H_2S	(75–4000) [69]; (1.3–70) [70]	None
CO_2	(2–50) [41]; (1–500) [47]; (1.2–403) [48]; (0.5–3000) [60]	None

tribution is very small in the intermediate- and high-energy regions. Consequently, the SCOP approach [11,12] is particularly suitable for those collision systems where the molecule possesses no dipole or quadrupole moment (for example, the CH_4 and SiH_4 molecules). The extension of the SCOP model to polar molecules [12] was also successful when anisotropic effects were included perturbatively in the first-order-Born approximation (FBA) in an incoherent manner. Thus, the results on the NH_3 and H_2O targets [12] were in very good agreement with available experimental data [25–33] at these intermediate and high energies. Note that the SCOP potential as such does not require any fitting procedure; however, it was possible to vary one parameter (Δ, the mean excitation energy of the target in the evaluation of absorption potential) in the calculation to bring theory and experiment even closer to each other. Nevertheless, the method [11,12] is capable of predicting quite reliable total cross sections without adjusting the Δ parameter, and thus produces theoretical results where no experimental data are available.

Trajmar, Register, and Chutjian [34] have summarized the experimental data on the electron-molecule systems through 1982. Recently, Stein and Kauppila [35], Szmytkowski [36], and Sueoka [37] have given a comprehensive list of references on the electron-molecule experimental σ_t data. In the following, we will exclude references pertinent to low-energy ($E \leq 20$ eV) collisions. A number of experiments have been performed to measure the σ_t at intermediate and high energies on several diatomic (H_2 [38–43], Li_2 [44], CO [45–49], N_2 [32,41,48,50–53], O_2 [52,54–58], and HCl [59]) and polyatomic (CO_2 [41,47,48,60], NH_3 [25–27], H_2O [27–33], C_2H_2 [61], CH_4 [43,57,62–69], H_2S [69,70], SiH_4 [71], CF_4 [69], and SF_6 [69], etc.) targets; however, no theoretical results are available to compare with these observed values except our own previous calculations on the CH_4, SiH_4, H_2O, and NH_3 molecules (see Refs. [11,12]). For some molecules (Li_2, HF, HCN, and PH_3) studied in this work, no experimental data in the present energy region could be found in the literature. In Table I, we have summarized the experimental and theoretical investigations made so far on the present list of molecules in the present energy range. It is clear from Table I that there is a paucity of theoretical work, even for the H_2 case.

The goal of this article is the following. First, we suggest a general and quite simple theoretical method that can predict σ_t values in a wide energy range for any molecular system for which Hartree-Fock-level wave functions are available. The other molecular quantities needed for the calculation are the polarizability, ionization potential, and various permanent multipole moments (dipole, quadrupole, etc.) of the isolated molecule. Second, we provide a simple fitted formula [see Eq. (16)] from our calculated data for the total cross section. Third, we provide Born-Bethe parameters [17–23] for all the molecules listed above. Fourth, we emphasize the fact that individual elastic (σ_{el}) and inelastic (σ_{abs}) (or absorption) cross sections (giving rise to the final σ_t quantity) should compare reasonably well with the corresponding experimental or more accurate theoretical results. For example, in the present case, our inelastic (or absorption) cross sections should be an upper bound to the experimental total ionization, electronic excitation, and dissociation channels together. There is evidence in the literature [16] that the final total cross section is in

good accord with the experiment, whereas the individual elastic and inelastic terms are not in good accord with the corresponding measured or calculated values.

Finally, we also examine the correlation between molecular and scattering parameters. A quantitative as well as qualitative correlation picture is presented that depicts several interesting aspects of electron-molecule scattering at high energies. In particular, the nuclear charge Z or the occupation number of the target play an important role in the values of σ_t for all the targets. Such correlations would allow us to better understand the scattering mechanism and to estimate cross sections for those molecules where experimental or theoretical studies are difficult to perform.

The basic philosophy of the present method is based on the assumption that the nonspherical nature (providing torque to the molecule for rotational excitation) of the molecular system does not play a significant role in shaping up the total cross section of the high-energy electron-molecule collisions. The collision time is too short and rotational excitation cross sections are insignificant relative to elastic, ionization, etc., processes. In addition, the contribution from the vibrational excitation process is assumed to be negligible. We, however, include these small anisotropic contributions (from dipole, quadrupole, etc., moments) to the total cross section in the FBA theory in an incoherent manner. It is to be noted here that the well-known independent-atom model (IAM) [72] for intermediate- and high-energy electron-molecule scattering is suitable for elastic scattering only. In the IAM procedure, the molecular behavior is included only via the internuclear geometry and the true nature of the molecular charge distribution is missing. At this time, a complex-optical-potential method appears to be a reliable and practical technique of predicting σ_t values for a large variety of molecules.

In the following two sections, we provide theoretical details and numerical procedures. The results are discussed in Sec. IV. The Born-Bethe parameters and correlations are examined in Sec. V, while concluding remarks are made in Sec. VI. We use atomic units in this paper unless otherwise specified.

II. THEORY

We first assume that the fixed-nuclei approximation is valid in this energy region and the interaction of the electron-molecule system can be represented by a local complex optical potential, namely,

$$V_{\rm opt}(\mathbf{r})=V_R(\mathbf{r})+iV_{\rm abs}(\mathbf{r}), \tag{1}$$

where the real part is a sum of three terms

$$V_R(\mathbf{r})=V_{\rm st}(\mathbf{r})+V_{\rm ex}(\mathbf{r})+V_{\rm pol}(\mathbf{r}) . \tag{2}$$

The static potential, $V_{\rm st}(\mathbf{r})$, is calculated from the unperturbed target wave function Ψ_0 at the Hartree-Fock level. The $V_{\rm pol}(\mathbf{r})$ represents approximately the short-range correlation and long-range polarization effects, while the $V_{\rm ex}(\mathbf{r})$ term accounts for electron exchange interaction. In this energy region, a local and real potential model for exchange and polarization effects is adequate. The $V_{\rm abs}$ in Eq. (1) is the absorption potential. Due to the nonspherical nature of a molecule, the optical potential [Eq. (1)] is not isotropic. A general expression for $V_{\rm opt}(\mathbf{r})$ for any target can be written in terms of the following multipole expansion around the center of mass (COM) of the molecule [73],

$$V_{\rm opt}^{p\mu}(\mathbf{r})=\sum_{l,h} v_{lh}(r)X_{lh}^{(p\mu)}(\hat{\mathbf{r}}) , \tag{3}$$

where $(p\mu)$ denotes the ground-state symmetry of the molecule and the symmetry-adapted X functions are defined in terms of real spherical harmonics $S_{lm}^{\pm}(\hat{\mathbf{r}})$ as [73,74]

$$X_{lh}^{(p\mu)}(\hat{\mathbf{r}})=\sum_{m=0}^{+l} b_{lhm}^{(p\mu)} S_{lm}^{q}(\hat{\mathbf{r}}) . \tag{4}$$

For closed-shell systems, the $(p\mu)$ is the totally symmetric [1] $^1A_1$ (nonlinear molecules) or $^1\Sigma_g^+$ (linear molecules) irreducible representation. The values of allowed l, h, m, etc., depend on a particular point-group symmetry of the molecule. The anisotropic terms, $l=1,2,\ldots,$ in expansion (3), provide torque to excite rotational levels in the molecule. As mentioned earlier, our main assumption in this work is that such higher-order terms are weak and can be treated separately in the first-order Born theory and added incoherently to the elastic part.

First we determine the target charge density $\rho(\mathbf{r})$ of a given molecule,

$$\rho(\mathbf{r})=\int |\Psi_0|^2 d\mathbf{r}_1 d\mathbf{r}_2 \ldots d\mathbf{r}_Z = 2\sum_{\alpha} |\phi_\alpha(\mathbf{r})|^2 , \tag{5}$$

where Z is the number of electrons in the target, ϕ_i is the ith molecular orbital, and a factor of 2 appears due to spin integration and an α sum being over each doubly occupied orbital. It can be shown that for closed-shell molecules, $\rho(\mathbf{r})$ belongs to a totally symmetric one-dimensional irreducible representation ($^1A_1$, $^1\Sigma_g^+$, or $^1\Sigma^+$) of the molecular point group [75]. All four potential terms ($V_{\rm st}$, $V_{\rm ex}$, $V_{\rm pol}$, and $V_{\rm abs}$) are functions of $\rho(\mathbf{r})$. For example,

$$V_{\rm st}(\mathbf{r})=\int \rho(\mathbf{r}_1)|\mathbf{r}-\mathbf{r}_1|^{-1} d\mathbf{r}_1 - \sum_{i=1}^{M} Z_i |\mathbf{r}-\mathbf{R}_i|^{-1} . \tag{6}$$

The $V_{\rm ex}$ is taken in the Hara free-electron gas-exchange (HFEGE) model [76] and $V_{\rm pol}$ is calculated in the correlation-polarization (COP) approximation [77–79]. Thus the accurate evaluation of $\rho(\mathbf{r})$ is important in our SCOP model. We employed various single-center expansion programs to determine the charge density and various potentials for linear [80] and nonlinear [81] molecules. The ALAM code of Morrison [80] was modified to include more than three nuclei; thus for the present C_2H_2 molecule, the modified version of ALAM (to be denoted here as MALAM [82]) generates single-center quantities of any planar molecule. For linear targets in this study, we obtained molecular wave functions from published tables [83], while for nonlinear cases we employed the MOLMON computer code [84]. In the present high-energy region, an exact representation of exchange-polarization correla-

tion is not important; thus the FEGE model for exchange and the COP approximation for polarization effects are accurate enough in these calculations.

The imaginary part of the optical potential $V_{\rm abs}(\mathbf{r})$ is the absorption potential, which represents approximately the combined effect of all the inelastic channels. An *ab initio* calculation of absorption potential is still an open problem. Here we employ a semiempirical absorption potential as discussed by Truhlar and co-workers [85]. The $V_{\rm abs}$ is a function of molecular charge density, incident electron energy, and the mean excitation energy Δ of the target. It is written as [85]

$$V_{\rm abs}(r)=-\rho(r)(v_{\rm loc}/2)^{1/2}(8\pi/5k^2k_f^3) \times H(k^2-k_f^2-2\Delta)(A_1+A_2+A_3)\ , \quad (7)$$

where

$$v_{\rm loc}(r)=k^2-V_{\rm st}(r)-V_{\rm ex}(r)-V_{\rm pol}\ , \quad (8a)$$

$$A_1=5k_f^3/2\Delta\ , \quad (8b)$$

$$A_2=-k_f^3(5k^2-3k_f^2)/(k^2-k_f^2)^2\ , \quad (8c)$$

$$A_3=2H(2k_f^2+2\Delta-k^2)\frac{(2k_f^2+2\Delta-k^2)^{5/2}}{(k^2-k_f^2)^2}\ , \quad (8d)$$

where $\frac{1}{2}k^2$ is the energy of the incident electron in hartrees. Here $H(x)$ is a Heaviside function defined by $H(x)=1$, for $x\geq 0$, and $H(x)=0$ for $x<0$. By varying the value of Δ in $V_{\rm abs}$ one can improve the absorption ($\sigma_{\rm abs}$) or σ_t cross sections relative to experimental or more accurate *ab initio* calculations; however, we have fixed Δ to be the ionization potential (I_p) of the molecule since the calculated value of Δ is very close to the ionization energy in most of the molecules (see Table II). In the case where our calculated Δ is very different from I_p (for example, the H_2 molecule, see below), we have given results with the same value of Δ, which has been used by other investigators. In most of the targets (except H_2), the use of I_p as Δ is good enough. This has reduced the uncertainty in the predicted cross sections, and moreover, the results do not change appreciably above a few hundred eV of energy. Full details of the $V_{\rm abs}$ potential in the present context of molecules are discussed elsewhere [11]. Here we consider only the spherical term in the single-center expansion of the absorption potential.

After generating the full optical potential [Eq. (1)] of a given electron-molecule system, we treat it exactly in a partial-wave analysis by solving the following set of first-order coupled differential equations for the real (χ_l) and imaginary ($\bar{\chi}_l$) parts of the complex phase-shift function under the variable-phase approach (VPA) [86],

$$\chi_l'(kr)=-\frac{2}{k}[2V_R(r)(A^2-B^2)+2V_{\rm abs}(r)AB], \quad (9)$$

$$\bar{\chi}_l'(kr)=-\frac{2}{k}[2V_R(r)AB-2V_{\rm abs}(r)(A^2-B^2)]\ , \quad (10)$$

where

$$A=\cosh\bar{\chi}_l(kr)[\cos\chi_l(kr)j_l(kr)-\sin\chi_l(kr)\eta_l(kr)]\ , \quad (11a)$$

$$B=-\sinh\bar{\chi}_l(kr)[\sin\chi_l(kr)j_l(kr)-\cos\chi_l(kr)\eta_l(kr)]\ , \quad (11b)$$

and $j_l(kr)$ and $\eta_l(kr)$ are the usual Riccati-Bessel functions [86]. Equations (9) and (10) are integrated up to a sufficiently large r different for different l and k values. Thus the final S matrix is written as

$$S_l(k)=\exp(-2\bar{\chi}_l)\exp(i2\chi_l)\ , \quad (12)$$

and the corresponding DCS's are defined as

$$\frac{d\sigma}{d\Omega}=\frac{1}{4k^2}\left|\sum_{l=0}^{l_{\max}}(2l+1)[S_l(k)-1]P_l(\cos\theta)\right|^2\ , \quad (13)$$

TABLE II. Various molecular properties used in this work. D, dipole moment; Q, quadrupole moment; α_0=polarizability; IP, ionization potential; B, rotational constant. For asymmetric top molecules, three (A, B, C), and for symmetric top molecules, two (A and B), values of rotational constants are given. All quantities are in atomic units unless the unit is specified.

Molecule	Z	α_0	D	Q	IP (eV)	Δ (eV)	B (cm^{-1})
H_2	2	5.417	0.0	0.494	15.43	4.87	60.85
Li_2	6	204.74	0.0	10.317	5.145	1.62	0.6726
HF	10	16.62	0.768	1.783	16.04	12.69	20.94
H_2O	10	11.0	0.780	2.580	12.0	11.0	27.88,14.51,9.28
NH_3	10	15.0	0.580	1.550	13.0	8.00	9.94,6.23
CH_4	10	17.50	0.0	0.0	12.98	10.50	5.242
N_2	14	11.80	0.0	−0.946	15.58	16.92	1.998
CO	14	13.16	0.099	−1.542	14.01	15.54	1.931
C_2H_2	14	22.5	0.0	5.365	11.41	11.82	1.174
HCN	14	17.0	1.266	1.774	13.85	13.27	1.478
O_2	16	10.70	0.0	−0.2547	12.07	21.20	1.446
HCl	18	17.80	0.471	2.829	12.75	9.80	10.593
H_2S	18	25.55	0.431	0.710	10.47	8.64	10.36,9.02,4.73
PH_3	18	32.67	0.523	−0.825	10.10	9.17	4.452,3.93
SiH_4	18	30.50	0.0	0.0	11.40	9.86	2.864
CO_2	22	17.90	0.0	−3.925	13.80	32.55	0.394

where $P_l(\cos\theta)$ is a Legendre polynomial of order l. The integrated elastic (σ_{el}), absorption (σ_{abs}), and σ_t cross sections are described in terms of the S matrix as follows:

$$\sigma_{el}^l=\frac{\pi}{k^2}(2l+1)|1-S_l(k)|^2,\quad \sigma_{el}=\sum_{l=0}^{l_{max}}\sigma_{el}^l \tag{14}$$

$$\sigma_{abs}^l=\frac{\pi}{k^2}(2l+1)[1-|S_l(k)|]^2,\quad \sigma_{abs}=\sum_{l=0}^{l_{max}}\sigma_{abs}^l \tag{15}$$

$$\sigma_t^l=\frac{2\pi}{k^2}(2l+1)[1-\mathrm{Re}S_l(k)],\quad \sigma_t^S=\sum_{l=0}^{l_{max}}\sigma_t^l\ . \tag{16}$$

We note that $\sigma_t^S=\sigma_{el}+\sigma_{abs}$ is the contribution from the spherical term only. In the above analysis the inelasticity or the absorption factor is defined by $|S_l(k)|=\exp(-2\bar{\chi}_l)$.

In order to include the contributions due to anisotropic terms (dipole, quadrupole, etc.) in the multipole expansion of the optical potential, we employ the FBA to evaluate the integral cross sections,

$$\sigma_{0\to J'}=\frac{2(2J'+1)}{k^2}\sum_{l,m}(2l+1)^{-1}\int_{|k-k'|}^{k+k'}dq\,q\left|\int_0^\infty dr\,r^2 v_{lm}(r)j_l(qr)\right|^2, \tag{17}$$

where dipole and quadrupole terms correspond, respectively, to $J'=1$ and 2 and the k' is the wave vector of the scattered electron [12]. For spherical top molecules (CH_4 and SiH_4), a spherical approximation is adequate to yield a reliable cross section [11,12]. Thus we write $\sigma_t=\sigma_t^S+\sigma_{0\to1}+\sigma_{0\to2}$. In addition, for all the molecules considered here, the contributions from octupole and higher-order moments can be neglected at such high energies without introducing any error at all. However, it becomes essential to consider the long-range dipole and quadrupole effects, in particular for polar molecules (HF, CO, HCN, HCl, H_2O, NH_3, PH_3, and H_2S). Such anisotropic terms are important below 100 eV impact energy. The CO molecule is very weakly polar whereas HCN is highly polar. It is to be noted here that the use of Eq. (17) in an incoherent manner may introduce some error in the final σ_t values, particularly below 100 eV. Consequently, our calculated total cross sections below 100 eV may be less accurate for those molecules possessing dipole and/or quadrupole moments. For this reason, we have given our cross sections with and without contributions from dipole and quadrupole terms.

It is to be noted here that in Eq. (17), we have employed our numerical values of the $v_{lm}(r)$ potential terms rather than use the asymptotic form only. Thus the integrals in Eq. (17) are done numerically. We have found [87] that there are significant differences in the FBA quantities (differential, total, and momentum-transfer cross sections) if calculated with or without the correct short-range behavior of the dipole, quadrupole, etc., potential terms. In the low-energy region, the small r region is not important due to the fact that higher-order partial waves are unable to penetrate the scattering region; however, in the present energy region, a large number of partial waves contribute to the scattering parameters and a correct short-range behavior of the potential is necessary in order to make appropriate use of the FBA theory.

III. NUMERICAL DETAILS

In order to solve Eqs. (9) and (10), we need a large number of partial waves [l_{max} in Eqs. (13)–(16)] in the present intermediate- and high-energy regions. We carried out convergence tests with respect to radial distance and the step size to preserve numerical accuracy. The value of l_{max} varied from 20 to 400, depending upon the impact energy. It was found that the higher-order VPA phase shifts ($l\geq30$) agree within 0.1% accuracy with the polarized Born calculations [88], using only the asymptotic form of the polarization potential. At each energy and for all the molecules considered here, the cross sections presented are fully converged with respect to increasing l_{max} and, where required, we switched from VPA phase shifts to polarized Born ones. In the special case of the Li_2 molecule with a very high value of polarizability (see Table II), we made sure that the integration was done properly to account for the long-range part of the interaction completely. We now discuss our results on the cross sections.

IV. RESULTS AND DISCUSSION

Before we discuss our cross sections, we first display the full optical potential [Eq. (1)] for a few selected molecules (H_2, Li_2, HF, N_2, H_2S, and CO_2) in Figs. 1 and 2. Figures 1(a) and 1(b) show the real part (V_R) at 100 eV (only the V_{ex} term is very weakly energy dependent), while the V_{abs} data are plotted in Figs. 2(a)–2(f) for the same set of molecules at a few selected energies. As expected, the V_{abs} is not a long-range effect and its penetration towards the origin increases with an increase in energy; this means that at high energies, the absorption potential takes into account the inner-shell excitation or ionization processes that may be closed at lower energies.

In the following, we have divided our discussion in terms of the isoelectronic sequence of molecules, because there are some similarities in the cross sections for isoelectronic molecules. Thus we have two-electron (H_2), six-electron (Li_2), ten-electron (HF, CH_4), 14-electron (CO, N_2, C_2H_2, and HCN), 16-electron (O_2), 18-electron (HCl, H_2S, PH_3, and SiH_4), and 22-electron (CO_2) systems to be discussed in the Secs. IV A–IV G.

A. The two-electron system: H_2

The H_2 molecule is the simplest neutral molecular system that has been studied extensively in the laboratory to determine σ_t values (see Table I). It is surprising that there exist very few calculations on this system for the σ_t above the ionization threshold. Van Wingerden, Wagenaar, and de Heer [13] performed semiempirical results at 20–2000 eV against their own experimental data, while Staszewska, Schwenka, and Truhlar [14] employed a laboratory-frame close-coupling scheme to determine σ_{el}, σ_{abs}, and σ_t values at 10, 40, and 100 eV. Their [14] results included the effects of nonspherical terms in a proper manner. The only other calculation on the e-H_2 σ_t cross-sections is by Liu [16], who employed the Born-Bethe-type theory in the energy range of 100–2000 eV. His σ_t values at these energies compare very well with the measurements; however, the individual terms (σ_{el} and σ_{abs}) differ significantly with other theoretical and experimental data.

As mentioned earlier, we use I_p instead of Δ in the evaluation of V_{abs} for all the molecules considered here. This assumption is based on the fact that the difference between the calculated value of Δ ($\Delta = 2\langle\Psi_0|z^2|\Psi_0\rangle/\alpha_0$) and the I_p is not significant for most of the molecules discussed in this work (see Table II). However, for the e-H_2 case, our values of Δ and I_p are, respectively, 4.86 and 15.43 eV. We therefore present our σ_t results by calculating V_{abs} with an intermediate value $\Delta = 10.6$ eV (solid curve in Fig. 3). and 15.43 eV (dashed curve in Fig. 3). The value of $\Delta = 10.6$ eV, also used by Staszewska, Schwenka, and Truhlar [14], is the difference between the ground state of H_2 and its first excited state. Note that both the theoretical curves in Fig. 3 include quadrupole contributions [Eq. (17)] in the FBA. As expected, the present SCOP model is reliable roughly above 100 eV; however, we see its fortuitous success up to 30 eV (Fig. 3). At 100 (40) eV, our σ_t value is 2.86 (4.65), which can be compared with the value of 2.73 (3.98), as calculated by Staszewski, Schwenka, and Truhlar [14].

The individual components σ_{el} and σ_{abs} are given in Tables III(a) and IV(a), respectively. There are a large number of experimental and theoretical data (see Refs. [1] and [34]) on the σ_{el} parameter. Our σ_{el} (see Table III(a)) values are in reasonable agreement with available experimental results [89–92] (not shown). For example, at 100 eV our 0.95 value is very close to the experimental values of 0.89 (Ref. [91]) and 0.77 (Ref. [92]). Our σ_{abs} curve for H_2 (Table IV(a)) exhibits a peaking behavior around 45 eV, which is in agreement with the behavior of of the total ionization cross section for the e-H_2 system [93]. In addition, there is good agreement between our σ_{abs} values and the calculation of Ref. [14]. In addition, our $\sigma_{0\to 2}$ value in the FBA approximation is in reasonable agreement with the calculations of Staczewska, Schwenka, and Truhlar [14].

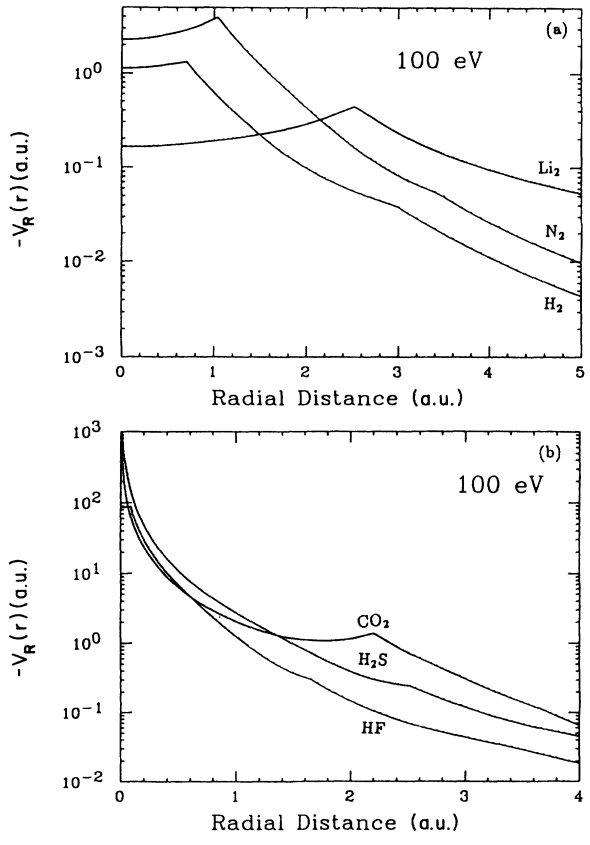

FIG. 1. (a) Real part of the complex-spherical-optical potential for electron scattering with H_2, Li_2, and N_2 systems. (b) Same legend as in (a) but for the HF, H_2S, and CO_2 cases.

B. The six-electron system: Li_2

We have considered the $^1\Sigma_g^+$ ground-state wave function of the Li_2 molecule from the published tables [83]. The values of polarizabilities ($\alpha_0 = 204.74a_0^3$, $\alpha_2 = 45.41a_0^3$) are taken from Ref. [94]. The contributions from the anisotropic polarizability and quadrupole terms $[(Q/r^3 + \alpha_2/r^4)P_2(\cos\theta)]$ is added incoherently in the FBA theory. In Fig. 4, we have shown σ_t values with and without nonspherical contributions. Above 100 eV, the contribution from anisotropic terms is small. There are no experimental data on this system in the present energy region. At 10 eV only, we can compare our σ_t value of $316.8a_0^2$ with the experimental [44] value of $350.0 \pm 105.00a_0^2$. The close-coupling calculations of Padial [95] for the e-Li_2 elastic scattering gives a value of $172.0a_0^2$, as compared to our value of $280.5a_0^2$. This indicates that at such low energy, the present prescription of adding an anisotropic contribution incoherently overestimates the elastic cross section. The results on the σ_{el} and σ_{abs} are given in Tables III(a) and IV(a), respectively. These cross sections decrease smoothly with energy except the absorption cross section, which has a peak around 30 eV.

C. The ten-electron systems: HF, H_2O, NH_3, and CH_4

For this isoelectronic sequence of closed-shell molecules, we have already reported SCOP calculations on the

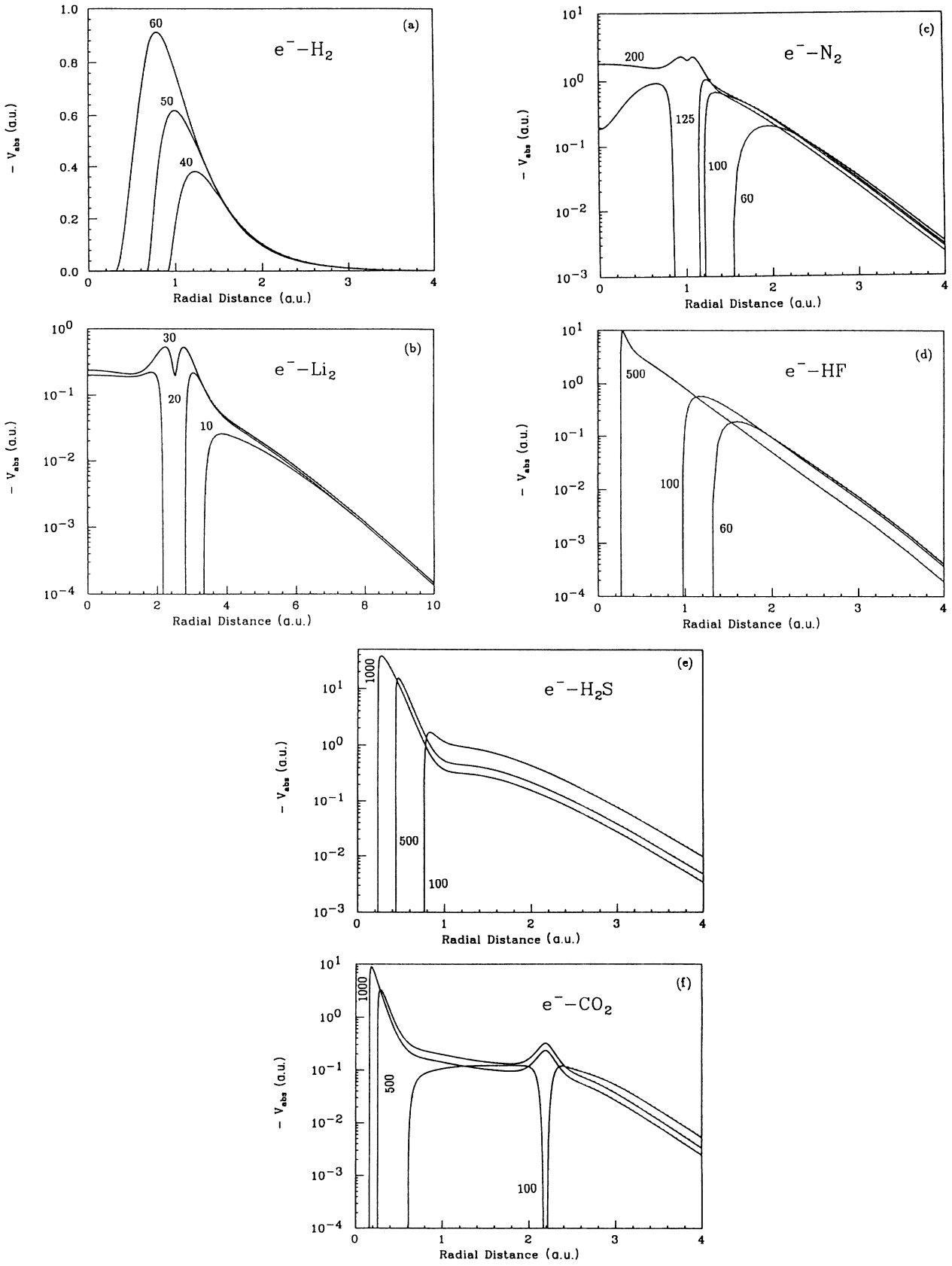

FIG. 2. (a) Imaginary part of the complex-spherical-optical potential for electron collisions with a H_2 molecule. The energy of each curve is shown in the figure in eV units. (b) Same as (a) but for the Li_2 target. (c) Same as (a) but for the N_2 targets. (d) Same as (a) but for the HF targets. (e) Same as (a) but for the H_2S molecule. (f) Same as (a) but for the CO_2 molecule targets.

H_2O, NH_3 (100–3000 eV) [12], and CH_4 (0.1–500 eV) [11] molecules. Here we supplement our earlier e-CH_4 results up to 5000 eV and compare them with very recent unpublished measurements of Nishimura and Sakae [68], and Karwasz and Zecca [69] in Fig. 5(a). Also shown in Fig. 5(a) are the experimental points of Dababneh *et al.* [57] and Floeder *et al.* [65]. Within the experimental error bars (not shown), our calculated values agree very

TABLE III. Elastic (σ_{el}) cross sections (in units of 10^{-16} cm^2) for various molecules at 10–5000 eV.

E (eV)	H_2	Li_2	HF	CH_4	N_2	CO	C_2H_2
			a				
10	8.551	78.522	22.692	20.717	27.059	34.236	41.736
20	5.334	36.532	14.014	16.312	22.036	23.761	32.660
30	3.000	23.261	10.467	11.881	20.685	21.789	26.900
40	2.179	18.339	8.436	8.864	19.241	19.842	22.321
50	1.705	15.526	7.107	6.919	17.461	17.720	18.692
60	1.397	13.506	6.166	5.691	15.573	15.691	16.024
70	1.194	11.939	5.465	4.834	13.780	13.938	14.059
80	1.060	10.676	4.923	4.226	12.219	12.488	12.490
90	0.958	9.635	4.491	3.817	11.074	11.283	11.550
100	0.874	8.768	4.138	3.520	10.109	10.292	9.762
125	0.713	7.115	3.483	3.011	7.978	7.872	7.764
150	0.599	5.950	3.025	2.665	6.521	6.312	6.481
175	0.514	5.089	2.680	2.402	5.412	5.397	5.730
200	0.450	4.432	2.398	2.194	4.862	4.839	5.184
300	0.296	2.870	1.705	1.650	3.598	3.614	3.822
400	0.220	2.085	1.377	1.334	2.914	2.922	3.040
500	0.174	1.619	1.172	1.124	2.453	2.455	2.522
600	0.144	1.310	1.028	0.975	2.118	2.117	2.155
700	0.123	1.092	0.916	0.861	1.863	1.860	1.880
800	0.107	0.931	0.830	0.773	1.662	1.658	1.667
1000	0.086	0.710	0.699	0.641	1.368	1.362	1.359
2000	0.042	0.409	0.396	0.352	0.723	0.718	0.703
3000	0.028	0.257	0.280	0.246	0.491	0.487	0.472
4000	0.021	0.195	0.222	0.191	0.371	0.368	0.355
5000	0.017	0.146	0.184	0.154	0.298	0.295	0.279
			b				
E (eV)	HCN	O_2	HCl	H_2S	PH_3	SiH_4	CO_2
10	79.088	32.100	32.956	48.512	51.876	48.849	55.780
20	54.384	25.656	25.124	32.200	30.589	30.920	47.558
30	41.865	24.361	18.986	20.485	20.403	20.590	37.811
40	34.192	22.135	15.878	15.036	14.712	13.720	31.908
50	28.742	19.561	14.000	11.532	10.479	10.452	26.804
60	24.560	17.070	12.675	8.738	8.739	8.978	21.770
70	21.333	14.861	11.601	7.473	7.766	8.070	17.478
80	18.860	13.044	10.630	6.696	7.088	7.408	14.932
90	16.923	11.640	9.854	6.102	6.564	6.884	13.263
100	15.287	10.260	9.249	5.645	6.135	6.451	12.166
125	12.026	7.915	8.150	4.821	5.328	5.621	10.512
150	9.974	6.628	7.365	4.246	4.746	5.014	9.454
175	8.538	5.727	6.752	3.870	4.299	4.543	8.645
200	7.594	5.126	6.253	3.439	3.939	4.160	7.983
300	5.408	3.810	4.900	2.625	2.993	3.150	6.152
400	4.236	3.060	4.086	2.172	2.440	2.558	5.032
500	3.485	2.556	3.525	1.866	2.070	2.168	4.265
600	2.962	2.193	3.120	1.645	1.807	1.894	3.706
700	2.576	1.919	2.810	1.473	1.612	1.693	3.280
800	2.279	1.706	2.566	1.339	1.462	1.539	2.944
1000	1.853	1.394	2.205	1.150	1.253	1.318	2.446
2000	0.958	0.725	1.375	0.742	0.790	0.817	1.337
3000	0.646	0.489	1.030	0.568	0.594	0.603	0.923
4000	0.487	0.368	0.834	0.471	0.481	0.481	0.706
5000	0.391	0.296	0.699	0.396	0.400	0.402	0.588

well with the observed data. In particular, in the keV energy region, our values are in excellement agreement with the recent unpublished data of Karwasz and Zecca [69]. The individual σ_{el} and σ_{abs} cross sections are presented in Tables III(a), and IV(a), and Table V(a).

Figure 5(b) present the *e*-HF cross sections with (solid curve) and without (dashed curve) the contributions from anisotropic (dipole and quadrupole) terms. No previous

TABLE IV. Absorption (σ_{abs}) cross sections (in units cm^{-16} cm^2) for various molecules at 10–5000 eV.

a

E (eV)	H_2	Li_2	HF	CH_4	N_2	CO	C_2H_2
10		9.631					
20	0.076	14.740	0.068	0.573	0.153	0.384	1.519
30	1.478	14.932	0.566	2.132	1.010	1.579	4.302
40	1.811	13.641	1.022	3.465	1.842	2.536	5.923
50	1.935	12.453	1.344	4.271	2.467	3.160	6.502
60	1.962	11.472	1.555	4.614	2.923	3.513	6.516
70	1.921	10.648	1.685	4.704	3.236	3.667	6.324
80	1.824	9.945	1.762	4.637	3.415	3.701	6.104
90	1.717	9.330	1.802	4.481	3.414	3.680	5.678
100	1.615	8.789	1.818	4.230	3.380	3.622	5.823
125	1.397	7.676	1.802	3.860	3.359	3.694	5.403
150	1.227	6.811	1.751	3.485	3.276	3.622	5.032
175	1.093	6.116	1.690	3.173	3.162	3.449	4.658
200	0.984	5.546	1.628	2.912	3.031	3.250	4.333
300	0.704	4.008	1.361	2.196	2.436	2.604	3.393
400	0.547	3.106	1.146	1.769	2.022	2.170	2.795
500	0.448	2.517	0.990	1.484	1.726	1.860	2.377
600	0.379	2.104	0.872	1.280	1.505	1.628	2.068
700	0.328	1.800	0.781	1.127	1.334	1.447	1.832
800	0.290	1.568	0.708	1.008	1.198	1.303	1.643
1000	0.234	1.236	0.597	0.834	0.995	1.086	1.365
2000	0.120	0.715	0.341	0.451	0.538	0.592	0.735
3000	0.080	0.465	0.241	0.308	0.367	0.405	0.496
4000	0.060	0.343	0.186	0.233	0.278	0.306	0.370
5000	0.048	0.263	0.152	0.176	0.223	0.246	0.271

b

E (eV)	HCN	O_2	HCl	H_2S	PH_3	SiH_4	CO_2
10							
20	0.317	0.652	0.655	1.778	3.056	2.179	0.500
30	1.601	1.941	2.076	3.945	5.995	5.672	2.185
40	2.765	2.880	3.091	5.177	7.356	7.946	3.735
50	3.513	3.469	3.656	5.792	8.074	8.306	5.001
60	3.963	3.851	3.944	6.244	7.822	7.965	6.332
70	4.158	4.110	4.126	6.125	7.417	7.523	7.331
80	4.178	4.242	4.261	5.882	7.017	7.094	7.632
90	4.116	4.259	4.246	5.627	6.649	6.701	7.690
100	4.052	4.325	4.145	5.385	6.316	6.346	7.578
125	3.960	4.278	3.812	4.852	5.614	5.600	7.070
150	3.788	4.086	3.498	4.417	5.059	5.018	6.545
175	3.621	3.905	3.228	4.058	4.612	4.555	6.070
200	3.406	3.712	2.998	3.758	4.246	4.178	5.654
300	2.715	3.061	2.351	2.927	3.252	3.169	4.426
400	2.253	2.606	1.953	2.418	2.661	2.580	3.631
500	1.925	2.268	1.682	2.073	2.265	2.189	3.078
600	1.680	2.007	1.484	1.821	1.981	1.911	2.673
700	1.490	1.800	1.333	1.629	1.766	1.703	2.363
800	1.339	1.631	1.213	1.477	1.599	1.540	2.118
1000	1.114	1.374	1.032	1.254	1.352	1.296	1.756
2000	0.603	0.766	0.610	0.735	0.783	0.741	0.951
3000	0.412	0.529	0.439	0.528	0.554	0.515	0.645
4000	0.311	0.404	0.344	0.413	0.427	0.391	0.483
5000	0.249	0.325	0.285	0.339	0.325	0.313	0.363

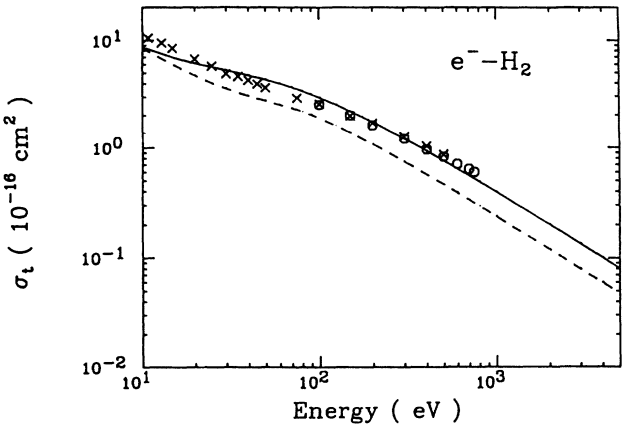

FIG. 3. Total (σ_t) cross sections for electron-H_2 scattering at 10–5000 eV. Theory: present SCOP results including the quadrupole contribution with $\Delta = 10.6$ eV (——) and $\Delta = IP$ (15.46 eV) (— — —). The experimental points are taken from Hoffman *et al.* [41] (×) and van Wingerden, Wagenaar, and de Heer [13] (○).

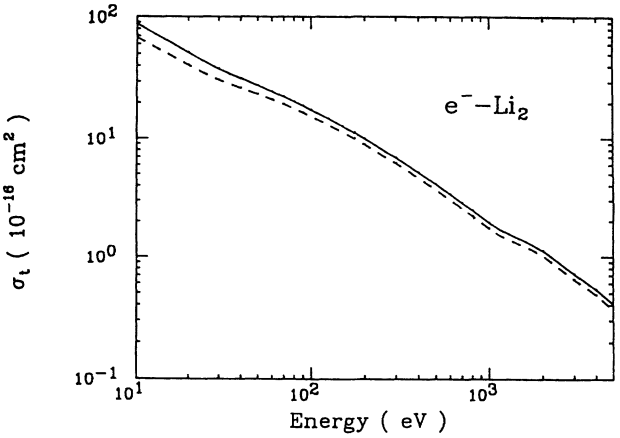

FIG. 4. Total (σ_t) cross section for electron-Li_2 scattering with (——) and without (— — —) the nonspherical-term contribution [Eq. (17)].

data, experimental or theoretical, are available for the HF molecule in the present energy region except the low-energy (0–15 eV) *e*-HF calculations that have been performed by Jain and Norcross [96] in the exact-static-exchange plus polarization model [we have not shown these results in Fig. 5(b) for obvious reasons]. As expected, the anisotropic terms contribute appreciably up to 500 eV energy. In Tables III(a) and IV(a) we have provided the σ_{el} and σ_{abs} cross sections, respectively, in the present energy range. The absorption cross sections are characterized by a peak around 100 eV. It is interesting to note that the inelastic cross section (σ_{abs}) is quite weak in this polar molecule as compared to the nonpolar CH_4 case.

D. The 14-electron systems: N_2, CO, C_2H_2, and HCN

At low energies, this isoelectronic sequence of molecules is known to exhibit a shape-resonance phenomenon around 2 eV due to the $^2\Pi$ (or $^2\Pi_g$) symmetry of the electron-molecule complex. At higher energies also, we see a clear similarity in their σ_t cross sections, plotted in Figs. 6(a)–6(d). No previous data, experimental or theoretical, could be found for the HCN molecule in the present energy region. However, for the CO and N_2 cases, there are several measurements (see Table I) included in Figs. 6(a), (N_2); 6(b), (C_2H_2); and 6(c), (CO). Above roughly 300 eV for the N_2 and CO gases, our calculations compare very well with all the experimental points, whereas below 300 eV, this agreement is only satisfactory. It appears from Figs. 6(a), 6(b), and 6(c) that the inclusion of an anisotropic contribution in the σ_t of N_2 and CO molecules has worsened the SCOP results. We see a weak shape-resonance behavior around 40 eV in both the N_2 and CO curves, while for the polar HCN molecule no such structure is observed. The CO molecule is almost a homonuclear (due to very weak dipole moment) and behaves similar to N_2 and C_2H_2 molecules. The experimental data of Kwan *et al.* [47] confirm this

TABLE V. Born-Bethe parameters [Eq. (18)] and the fitted parameters for σ_t [Eq. (19)] for various molecules.

Mol.	A_{el}	B_{el}	C_{el}	M^2_{tot}	$\ln(C_{tot})$	a'	b'	c'
H_2	6.988	8.287	46.873	0.1386	29.151	−0.0484	−16.261	7.088
Li_2	66.052	−605.136	24010.7	1.2335	16.087	0.7509	−36.319	40.266
HF	80.127	−2089.41	35368.9	2.405	−0.596	4.1656	−118.370	10.675
H_2O	77.078	−1061.74	12539.9	2.8823	−1.9982	3.2344	−121.895	14.595
NH_3	69.689	−769.396	7657.0	3.039	−0.999	3.4825	−93.766	15.702
CH_4	67.071	−1258.73	19344.1	1.55	5.299	2.2206	−155.207	23.302
N_2	127.142	−1026.77	3901.234	2.340	3.334	0.4047	−413.093	53.137
CO	125.671	−930.713	2444.26	2.6813	2.5257	0.3592	−446.945	55.607
C_2H_2	118.705	−292.386	−8197.65	2.0901	7.4713	−3.5937	−690.106	82.064
HCN	165.057	−843.819	4078.26	2.5477	3.1816	0.3619	−401.121	65.757
O_2	124.959	−629.306	−1981.92	4.4329	0.5782	0.9867	−512.541	60.423
HCl	316.545	−13150.0	2.69039^{+5}	5.3459	−1.6863	23.033	171.416	−33.632
H_2S	181.278	−8630.43	1.8224^{+5}	6.1012	−1.4263	18.239	238.458	−31.286
PH_3	183.115	−7879.91	1.6244^{+5}	5.1835	−0.3260	17.907	232.739	−25.796
SiH_4	182.389	−8630.43	1.8224^{+5}	4.4932	0.2197	14.793	68.171	−9.989
CO_2	251.089	−4296.19	60080.0	3.0775	5.8837	2.2156	−768.418	88.814

weak feature around 30–40 eV for the N_2 and CO molecules. In fact, almost all measurements on the CO and N_2 systems exhibit this broad resonance effect above the ionization threshold. It has been suggested that a broad intermediate-energy shape resonance of σ_u symmetry occurs in the case of e-N_2 scattering [97]. There is an indication of this intermediate-energy broad feature in other nonpolar molecules also, such as the O_2 and CO_2 molecules (see below). The HCN target is a strongly polar molecule and therefore the low-energy cross sections ($E \leq 100$ eV) are dominated by the dipole scattering.

Above 100 eV, we see excellent agreement between theory and experiment for these isoelectronic molecules (CO, N_2, and C_2H_2). The individual elastic and absorption cross sections for all four molecules are given in Tables III and IV. The absorption cross-section peak in the e-N_2 case, around 90 eV, is in good agreement with the measured total ionization cross-section behavior (see Ref. [93]). In general, N_2 and CO have similar σ_{el} and σ_{abs} values. The C_2H_2 has the largest absorption cross sections as compared to the HCN, CO, and N_2 cases. The HCN molecule has the largest σ_{el} values among the four molecules.

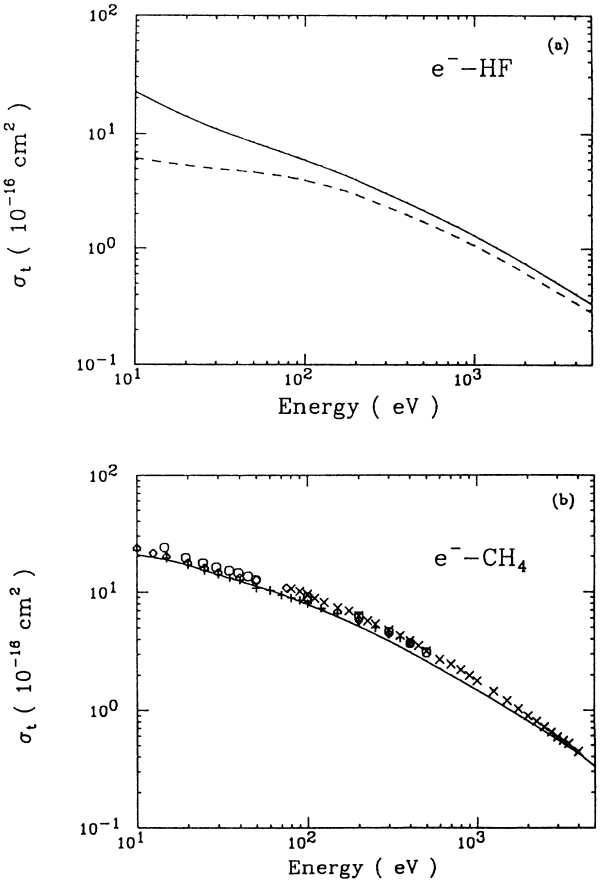

FIG. 5. Total cross sections for the isoelectronic CH_4 and HF molecules at 10–5000 eV. The solid curve is the present SCOP calculations. (a) For the e-HF case, the solid and dashed curves are, respectively, with and without anisotropic contributions [dipole and quadrupole contributions, Eq. (17)]. (b) For CH_4, the experimental points are taken from: ×, Ref. [69]; ○, Ref. [57]; ◇, Ref. [65]; +, Ref. [66].

E. The 16-electron system: O_2

The O_2 molecule is an open-shell molecule and its ground-state ($^3\Sigma_u^-$) wave function is taken from the tables of Cade and Wahl [98]. In this intermediate- and high-energy region, the effects of singlet or triplet states are not important. There are several experimental measurements available for the e-O_2 total cross sections (see Table I), whereas there are no theoretical results except the Born-Bethe calculation of Liu [16]. In Fig. 7, we have plotted our σ_t values at 10–5000 eV along with the measurements of Dalba *et al.* [52] and Dababneh *et al.* [57]. We see a very good agreement between our values and the observed ones. The Born-Bethe results of Liu [16] are also shown for comparison. We immediately notice that the present SCOP total cross sections are more reliable even at those energies ($E \geq 1600$ eV) where no other data, experimental or theoretical, could be found in the literature. It is to be noted here that at the lower end of the present energy region, the first-order Born theory may not be valid, as is clear from a comparison of the Born-Bethe results of Liu [16]. As noticed earlier, we also see here that the pure spherical terms compare better than the full (spherical plus nonspherical) results. This may be partly due to the approximation treatment of nonspherical terms as well as the accuracy of experimental data.

Our σ_t^S results in Fig. 7 exhibit a broad structure around 40 eV (dashed curve), while in the σ_t (solid line) cross section this feature appears around 30 eV. The experimental points of Dababneh *et al.* [57] and Zecca *et al.* [56] confirm this behavior. It may be a weak shape-resonance effect or it may arise mainly from inelastic channels. Below 100 eV, various experimental σ_t agree with each other within roughly 20%.

In Tables III(b) and IV(b), the σ_{el} and σ_{abs} values are given. The peaking behavior in the σ_{abs} parameter around 100 eV is in agreement with the experimental total ionization cross section [93]. The elastic cross sections [Table III(b)] compare very well with other theoretical results [99] (not shown).

F. The 18-electron systems: SiH_4, HCl, PH_3, and H_2S

Here the experimental data are available for HCl [59], SiH_4 [71], and H_2S [69,70] molecules (see Table I for energy range). The present SiH_4 results are supplementary to our previous results [11], reported only up to 500 eV. In Figs. 8(a)–18(d), we have plotted the σ_t for all the four gases along with the available experimental data. It is clear from these figures that the present results above 100 eV are in very good agreement with observed data. In particular, our calculations compare well with very recent unpublished measurements Karwasz and Zecca [69] for the e-H_2S case from 75 to 4000 eV. The agreement for HCl and SiH_4 cases with the experiments of Sueoka

and co-workers is also very good, particularly above 50 eV. No intermediate-energy shape-resonance phenomenon is observed in any of the 18-electron systems as seen earlier for the 14-electron nonpolar gases. For the H_2S, HCl, and PH_3 cases, we have shown our calculations with and without anisotropic contributions [Eq. (14)]. As also seen in the previous sections, the contribution from dipole and quadrupole terms is insignificant above 100 eV. In the case of the H_2S molecule, the inclusion of the contribution from multipole moments has improved the SCOP results.

Finally, numerical values of the elastic and inelastic cross sections are shown separately in Tables III(b) and IV(b) for all the four molecules in the present energy regime (10–5000 eV). No other experimental or theoretical values could be found in the literature to compare to our numbers in Tables III(b) and IV(b) for these molecules. For the e-PH_3 absorption cross sections [Table IV(b)], the peaking behavior around 50 eV is in fair agreement with experimental total ionization and dissociation cross sections [100].

G. The 22-electron system: CO_2

The CO_2 molecule is a big molecule from an *ab initio* electron-molecule scattering point of view. The theoretical studies on the e-CO_2 scattering are scarce. The experimental σ_t are available up to 3000 eV (see Table I). In Fig. 9, we have compared our SCOP σ_t results with three sets of experimental points [47,48,60]. Both curves, i.e., with and without nonspherical-terms contributions, are shown in Fig. 9. From Fig. 9, we see that below 100 eV, the agreement with experimental data becomes poor when the contribution from the anisotropic terms is added incoherently in the FBA. Even for this heavier system, our calculations prove to be very successful particularly above a few hundred eV. We see a slight structure around 30–40 eV similar to the N_2, CO, O_2, etc., molecules, but it is quite weak. Below 100 eV, our values are much higher than the measured ones; however, as expected, above 100 eV, we agree very well with the recent measurements of Kwan *et al.* [47] and Szmytkowski *et al.* [60]. The σ_{el} and σ_{abs} cross sections are provided in Tables III(b) and IV(b). The peaking structure around 100 eV in the σ_{abs} parameter is in agreement with experimental total ionization cross-section behavior [93].

For such a heavy and anisotropic system, our results are very encouraging and therefore we emphasize that at high energies a spherical charge-density description of the target accounts quite reliably for the total scattering

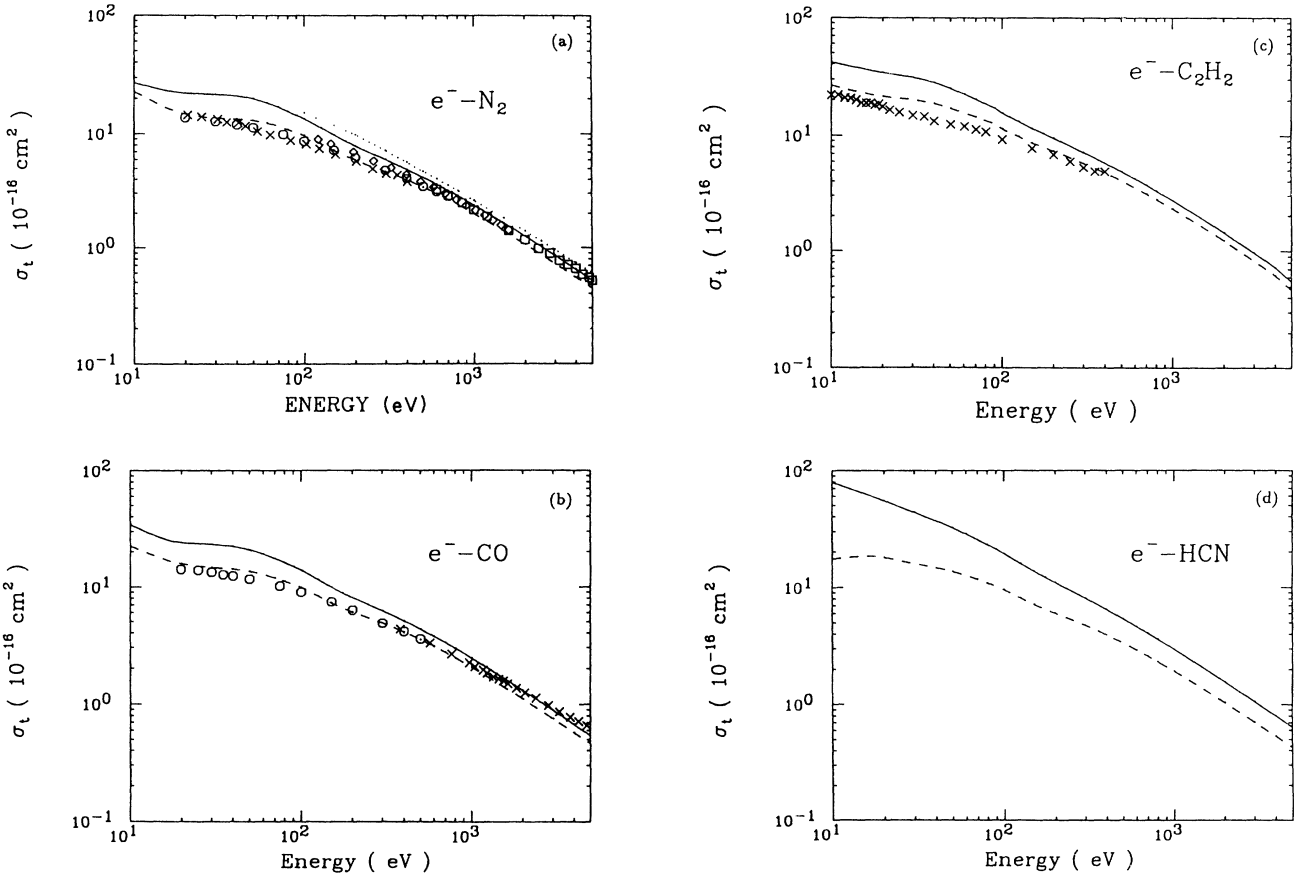

FIG. 6. Total cross sections for electron scattering with isoelectronic N_2, CO, C_2H_2 and HCN molecules in the range 10–5000 eV. Present calculations are shown with (——) and without (— — —) anisotropic-term contributions. (a) For N_2 the dotted curve is the Born-Bethe results of Liu [16]. Experiment: ◇, Ref. [52]; □, Ref. [53]; ○, Ref. [41]; ×, Ref. [48]. (b) For CO measurements are from Refs. [49] (×) and [47] (○). (c) For C_2H_2 measurements are taken from Ref. [61]. (d) is for HCN.

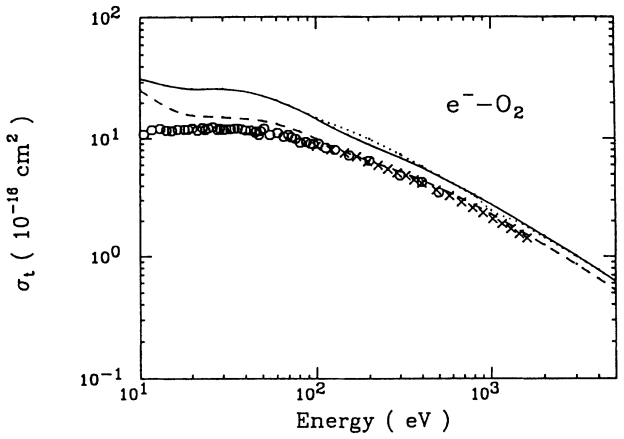

FIG. 7. Total cross sections for electron-O_2 scattering at 10–5000 eV in the present SCOP model with (——) and without (— — —) the contribution from the quadrupole term in the FBA. The dotted curve is the Born-Bethe calculations of Liu [16] starting at 100 eV. Experiment: ×, Ref. [52]; ○, Ref. [57].

process. It may be interesting to test the SCOP model for another 22-electron system N_2O where experiments have been performed on the σ_t parameter (see Ref. [26]).

V. DISCUSSION ON THE CORRELATION

A. The Born-Bethe parameters

In the preceding section, we have seen that the SCOP approximation is a reliable model above a few hundred eV energy. It will therefore be interesting to employ our high-energy cross sections (σ_{el}, σ_{abs}, and σ_t) to determine Born-Bethe parameters [17–24]. The Bethe theory defines the total inelastic (σ_{abs}) cross section, while the Born approximation gives the total elastic (σ_{el}) cross section. Thus a combined Born-Bethe theory expresses the total cross section in terms of the following analytic formula:

$$\frac{E}{R}\frac{\sigma_t}{\pi a_0^2} = \left[A_{rel} + B_{el}\frac{R}{E} + C_{el}\left[\frac{R}{E}\right]^2 \cdots \right] + \left[4M_{tot}^2 \ln\left[4C_{tot}\frac{E}{R}\right] + \cdots \right], \quad (18)$$

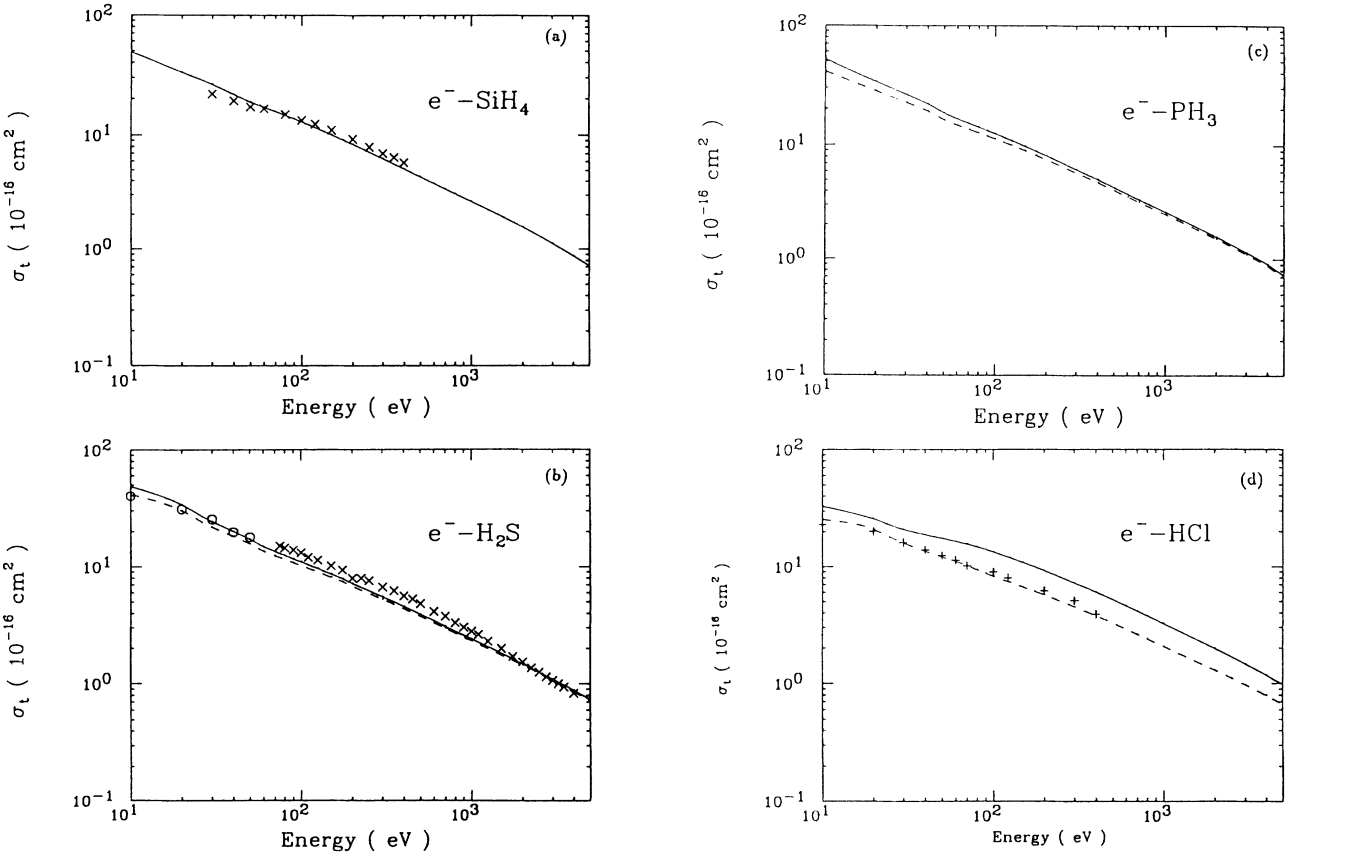

FIG. 8. Total cross sections for electron scattering with SiH_4, H_2S, PH_3, and HCl molecules at 10–5000 eV. (a) e-SiH_4 results in the SCOP model (——); ×, the measurements of Sueoka and Mori [71]. (b) e-H_2S results in the present SCOP model with (——) and without (— — —) the contributions from nonspherical (dipole plus quadrupole) terms. The experimental points are from Refs. [69] (×) and [70] (○). (c) For PH_3, the same as in (b). (d) For HCl, the same as in (b) with the experimental points (+) taken from Ref. [59].

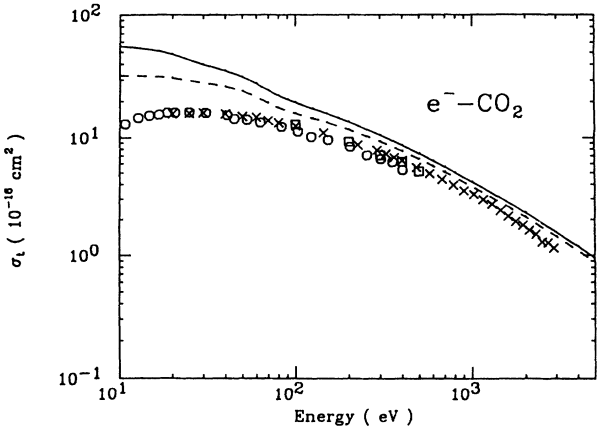

FIG. 9. Total cross sections for electron CO_2 scattering in the SCOP model at 10–5000 eV with (——) and without (— — —) the contribution from the quadrupole term. The experimental data are from Refs. [47] (□), Ref. [48] (○), and Ref. [60] (×).

where E is the incident energy in eV, R is the Rydberg energy, and a_0 is the Bohr radius. The constants A_{el}, B_{el}, C_{el}, M_{tot}, and C_{tot} have a physical significance and are given for several atomic systems in Ref. [21]. The M^2_{tot} is related to the optical oscillator strength of the molecule. Liu [16] has applied these atomic parameters to yield total cross sections for homonuclear molecules. However, these constants, available for some molecular systems to determine σ_t, are not accurate enough to agree with experimental data [53]. To our knowledge, there are hardly any results in the literature on the Born-Bethe parameters [Eq. (18)] for most of the molecules studied here. In addition, we fit a general formula for the σ_t from our calculated values in the following form:

$$\frac{E}{R}\frac{\sigma_t}{4\pi a_0^2} = a' \ln\frac{E}{R} + b'\frac{R}{E} + c' , \tag{19}$$

and provide the values of the constants a', b', and c' for the present set of molecules.

The Born-Bethe parameters [Eq. (18)] were evaluated from our σ_{el} and σ_{abs} results in the range of 500–5000 eV. From Table II, we have summarized some properties of the molecules used in the present calculation. In Table V, we have provided Born-Bethe [Eq. (18)] and a', b', and c' [Eq. (16)] parameters for all the molecules considered here. In Table V, we have also included parameters for the NH_3 and H_2O targets from the results of Ref. [12]. The c' and a' parameters in Eq. (19) determine the main component of σ_t.

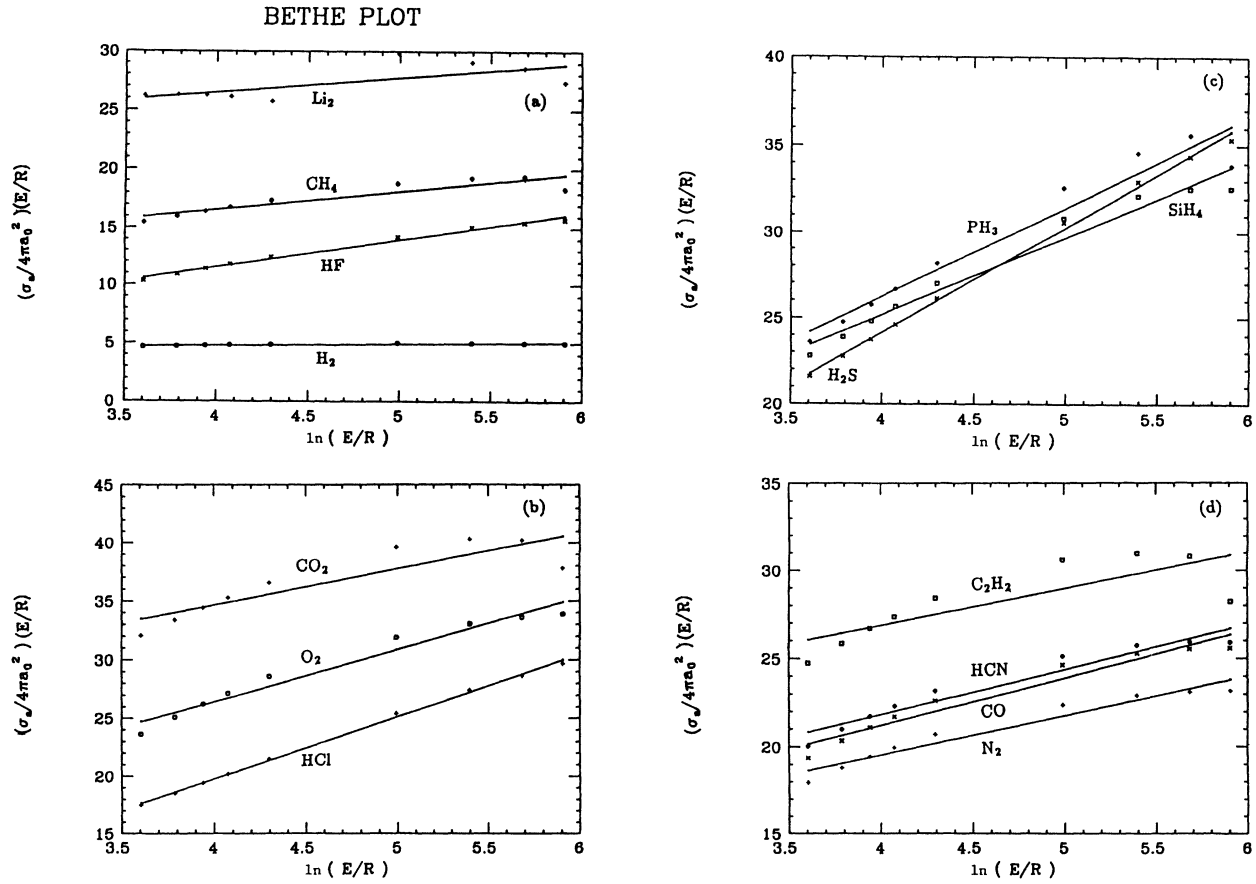

FIG. 10. (a) Bethe plots for H_2, HF, CH_4, and Li_2 molecules; (b) for HCl, O_2, and CO_2 molecules; (c) for H_2S, PH_3, and SiH_4 molecules; and (d) for N_2, CO, HCN, and C_2H_2 molecules.

In order to further analyze our total-cross-section results, we have made Bethe plots $[\sigma_{abs}E/(4\pi Ra_0^2)$ vs $\ln(E/R)]$ for all the molecules in Figs. 10(a)–10(d). According to the Bethe theory, the Bethe plot should be a straight line with a gradient of M_{tot}^2. We see from these figures [10(a)–10(d)] that our Bethe plot for each molecule is almost a straight line. The results inferred from the Born theory generally overestimate the experimental data [53]. For N_2 and CO molecules Garcia and co-workers (Refs. [49] and [53]) have determined Born-Bethe parameters. Our data given in Table V can be useful to compare with further theoretical and experimental results and also to extrapolate the total cross section at higher energies.

B. Correlation of σ_t with molecular properties

We further put together the above description of high-energy electron scattering with a variety of diatomic and polyatomic molecules. It is always useful to know the variation of cross sections in different targets. We have already seen that isoelectronic collisional systems possess similar cross sections both in quantity and quality. Except for very highly polarizable Li_2 or the simple H_2 molecules, we might expect some kind of correlation between σ_t and any molecular property (number of electrons Z, polarizability, multipole moments, molecular size, etc.). Very recently, Szmytkowski [36] has examined the trend of total cross sections at 100 and 50 eV in a large variety of atoms and molecules with respect to the target dipole polarizability. He [36] has observed some correlation of σ_t with the diamagnetic susceptibility and the number of electrons in the target.

As we have seen so far, a general feature above 100 eV, common for all the above targets, is the decrease of σ_t with an increase in impact energy. Floeder *et al.* [65] have also seen from their high-energy electron-scattering data for several hydrocarbon molecules that the total cross sections increase with the size of the molecule and, between 100–400 eV, the σ_t can be described as a linear function of Z, the number of molecular electrons. In Figs. 11(a) and 11(b), we have examined the value of σ_t as a function of Z and α_0, respectively. We have shown these data only at 1000 and 5000 eV, where the present model gives the best comparison with experiment. From Fig. 11(a), we can clearly see that the σ_t values increase with an increase in Z, i.e., there is a strong correlation between the total cross section and the size of the target. On the other hand, we do not see such a correlation with respect to target polarizability [Fig. 11(b)]. However, at lower energies (around 100 eV), the σ_t seems to have a strong dependence on α_0 (see Ref. [36]). From our σ_t–Z correlation diagram [Fig. 11(b)], a rough estimate of the total cross section can be made for any molecular system with Z smaller or even greater than 22.

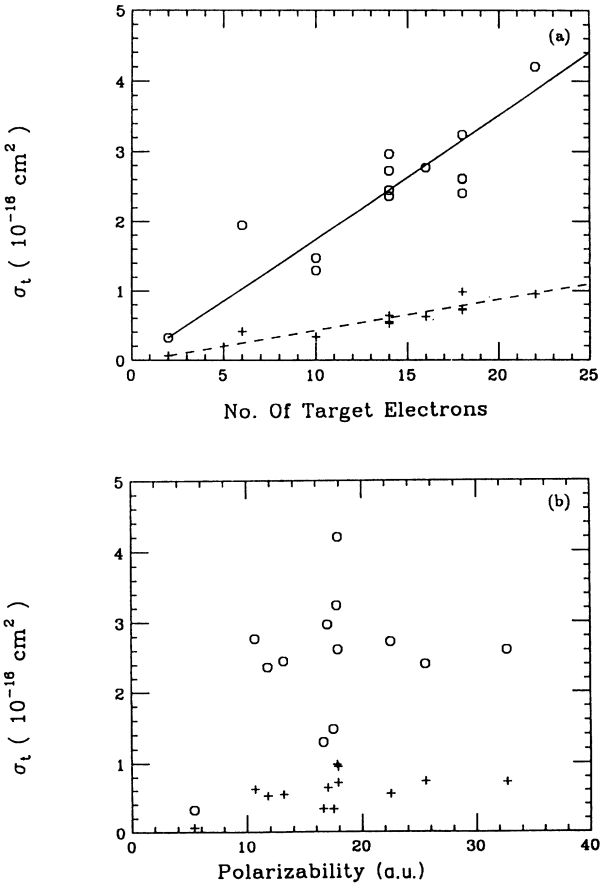

FIG. 11. (a) Variation of total cross section with the number of target electrons (Z). ○, at 1000 eV; +, at 5000 eV. (b) Variation of total cross sections with the target polarizability. ○, at 1000 eV; +, at 5000 eV.

VI. CONCLUSIONS

We have presented the total (elastic plus inelastic) cross sections of the intermediate- and high-energy electron impact with a large variety of molecules,where experimental studies have been carried out recently. A complex optical potential is derived for each system from target wave functions and its spherical part is employed to yield total cross sections under the complex phase-shift analysis. For the nonspherical part of the optical potential, we used the first-order Born approximation and added this contribution incoherently to the spherical part. We have avoided any kind of fitting procedure in the present calculation. The present model mainly requires the target charge density, polarizability, multipole moments, ionization potential, etc., of the molecule. At and above 100 eV, our results for all the molecules studied here are in very good agreement with available measurements. Below 100 eV, we have discussed the limitations of the present theory. It is worthwhile to mention that these results will fill the gap between theory and experiment and inspire some new experiments to be performed on certain molecules (for example, Li_2, HF, HCN, PH_3, etc.). For

C_2H_2, HCl, and SiH_4 molecules, only Sueoka, Mori, and Katayama [31] have performed σ_t measurements below 500 eV. We need more experimental data for these systems particularly in the keV energy region. We plan to investigate several other large molecules where experimental data exist (for example, SF_6, SO_2, N_2O, OCS, several hydrocarbons, NO, etc.). The method employed here is easy and practical and requires no prior information on the cross-section parameter. We [101] have extended this work for positron-molecule σ_t cross sections for several molecular gases where recent experimental data are available at intermediate and high energies.

ACKNOWLEDGMENTS

This research is funded by the U.S. Air Force, Wright-Patterson Air Force Base, under Contract No. FY33615-90-C-2032. This work is also partially supported by the U.S. Army Office of Scientific Research, under Contract No. DAAL03-89-9-0111. We thank the Florida State University Supercomputer Research Institute (SCRI) for providing supercomputing time. We are thankful to Dr. A. Zecca, Dr. R. S. Brusa, Dr. S. Oss, and Dr. G. Karwasz for providing us with their experimental σ_t data prior to publication.

*Permanent address: Department of Physics and Astrophysics, University of Delhi, Delhi 110007, India.

[1] *Electron Molecule Interactions and Their Applications,* edited by L. G. Christophorou (Academic, New York, 1984), Vols. 1 and 2.
[2] *Molecular Processes in Space,* edited by T. Watanabe *et al.* (Plenum, New York, 1990).
[3] A. V. Phelps, Ann. Geophys. **28**, 611 (1972).
[4] M. Hayashi, in *Swarm Studies and Inelastic Electron-Molecule Collisions,* edited by L. C. Pitchford *et al.* (Springer-Verlag, New York, 1985).
[5] M. Inokuti, in Argonne National Laboratory Report No. 84-28, 1983 (unpublished).
[6] N. F. Lane, Rev. Mod. Phys. **29**, 40 (1980); for a comprehensive list of review articles on electron-molecule collisions, see Ref. [1] above.
[7] *Electron Atom and Electron-Molecule Collisions,* edited by J. Hinze (Plenum, New York, 1983).
[8] *Aspects of Electron-Molecule Scattering and Photoionization,* edited by A. Herzenberg (AIP, New York, 1990).
[9] F. A. Gianturco and A. Jain, Phys. Rep. **143**, 325 (1986).
[10] R. L. Platzman, Int. J. Appl. Radiat. Isot. **10**, 116 (1961).
[11] A. Jain, Phys. Rev. A **34**, 3707 (1986); J. Chem. Phys. **86**, 1289 (1987).
[12] A. Jain, J. Phys. B **22**, 905 (1988).
[13] B. van Wingerden, R. W. Wagenaar, and F. J. de Heer, J. Phys. B **13**, 3481 (1980).
[14] G. Staczewska, D. W. Schwenka, and D. G. Truhlar, J. Chem. Phys. **81**, 335 (1984).
[15] Y. Itikawa, M. Hayashi, A. Ichimura, K. Onda, K. Sakimoto, K. Takayanagi, M. Nakamura, H. Nishimura, and T. Takayanagi, J. Phys. Chem. Ref. Data **15**, 985 (1986).
[16] J. W. Liu, Phys. Rev. A **35**, 591 (1987); **32**, 1384 (1985).
[17] H. Bethe, Ann. Phys. **5**, 325 (1930).
[18] H. Bethe, in *Handbuch der Physik,* edited by H. Geiger and K. Scheel (Springer, Berlin, 1933), Vol. X, p. 273.
[19] M. Inokuti, Y. K. Kim, and R. L. Platzman, Phys. Rev. **164**, 55 (1967).
[20] M. Inokuti, Rev. Mod. Phys. **43**, 297 (1971).
[21] M. Inokuti, R. P. Saxon, and J. L. Dehmer, J. Radiat. Phys. Chem. **7**, 109 (1975).
[22] M. Inokuti and M. R. C. McDowell, J. Phys. B **7**, 2382 (1974).
[23] M. Inokuti, Y. Itikawa, and J. E. Turner, Rev. Mod. Phys. **50**, 23 (1978).
[24] R. F. Egerton, *Electron Energy-Loss Spectroscopy in the Electron Microscope* (Plenum, New York, 1986).
[25] O. Sueoka, S. Mori, and Y. Katayama, J. Phys. B **20**, 3237 (1987).
[26] C. Szmytkowski, K. Maciag, C. Karwasz, and D. Filipkovic, J. Phys. B **22**, 525 (1989).
[27] E. Bruche, Ann. Phys. (Leipzig) **1**, 93 (1929).
[28] F. Schmieder, Z. Elektrochem. **36**, 700 (1930).
[29] A. Zecca, G. Karwasz, S. Oss, R. Grisenti, and R. S. Brusa, J. Phys. B **20**, L133 (1987).
[30] C. Szmytkowski, Chem. Phys. Lett. **136**, 363 (1987).
[31] O. Sueoka, S. Mori, and Y. Katayama, J. Phys. B **19**, L373 (1986).
[32] H. Nishimura and K. Yano, J. Phys. Soc. Jpn. **57**, 1951 (1988).
[33] Z. Saglam and N. Aktekin, J. Phys. B **23**, 1529 (1990).
[34] S. Trajmar, D. F. Register, and A. Chutjian, Phys. Rep. **97**, 219 (1983).
[35] T. S. Stein and W. E. Kauppila, in *Electronic and Atomic Collisions,* edited by D. C. Lorentz *et al.* (Elsevier, New York, 1986), p. 105.
[36] C. Szmytkowski, Z. Phys. D **13**, 69 (1989).
[37] O. Sueoka, in *Atomic Physics with Positrons,* edited by J. W. Humberston and E. A. G. Armour (Plenum, New York, 1987), p. 41.
[38] G. Dalba, P. Fornasini, I. Lazzizzera, G. Ranieri, and A. Zecca, J. Phys. B **13**, 2839 (1980).
[39] R. K. Jones, Phys. Rev. A **31**, 2898 (1985).
[40] M. S. Dababneh, Y. F. Hsieh, W. E. Kauppila, V. Pol, and T. S. Stein, Phys. Rev. A **26**, 1252 (1982).
[41] K. R. Hoffman, M. S. Dababneh, Y. F. Hsieh, W. E. Kauppila, V. Pol, J. H. Smart, and T. S. Stein, Phys. Rev. A **25**, 1393 (1982).
[42] A. Deuring, K. Floeder, D. Fromme, W. Raith, A. Schwab, G. Sinapius, G. Zitzewitz, and P. W. Krug, J. Phys. B **16**, 1633 (1983).
[43] E. A. Kurz, Ph.D. thesis, Indiana University, Bloomington, 1987.
[44] T. M. Miller, A. Kasdan, and B. Bederson, Phys. Rev. A **25**, 1777 (1982).
[45] E. Bruche, Ann. Phys. (Leipzig) **83**, 1065 (1927).
[46] C. Ramsauer and R. Kollath, Ann. Phys. (Leipzig) **10**, 143 (1931).
[47] Ch. K. Kwan, Y. F. Hsieh, W. E. Kauppila, S. J. Smith, T. S. Stein, M. N. Uddin, and M. S. Dababneh, Phys. Rev. A **27**, 1328 (1983).
[48] O. Sueoka and S. Mori, J. Phys. Soc. Jpn. **53**, 2491 (1984).
[49] G. Garcia, C. Aragon, and J. Campos, Phys. Rev. A **42**, 4400 (1990).
[50] R. E. Kennerly, Phys. Rev. A **21**, 1876 (1980).
[51] H. J. Blaauw, R. W. Wagenaar, and F. J. de Heer, J. Phys.

B **13**, 359 (1980).
[52] G. Dalba, P. Fornasini, R. Grisenti, G. Ranieri, and A. Zecca, J. Phys. B **13**, 4695 (1980).
[53] G. Garcia, A. Perez, and J. Campos, Phys. Rev. A **38**, 654 (1988).
[54] G. Sunshine, B. B. Aubrey, and B. Bederson, Phys. Rev. **154**, 1 (1967); A. Salop and H. H. Nakano, Phys. Rev. A **2**, 127 (1970).
[55] R. A. Bonham and R. E. Kennerly, Acta. Chim. Acad. Sci. Hung. **99**, 265 (1979).
[56] A. Zecca, R. S. Brusa, R. Cresenti, S. Oss, and C. Szmytkowski, J. Phys. B **19**, 3353 (1986).
[57] M. S. Dababneh, Y. F. Hsieh, W. E. Kauppila, Ch. K. Kwan, S. J. Smith, T. S. Stein, and M. N. Uddin, Phys. Rev. A **38**, 1207 (1988).
[58] K. P. Subramaniam and V. Kumar, J. Phys. B **23**, 745 (1990).
[59] O. Sueoka and A. Hamada, At. Coll. Res. Jpn. **16**, 18 (1990).
[60] C. Szmytkowski, A. Zecca, G. Karwasz, S. Oss, K. Maciag, B. Marinkovic, R. S. Brusa, and R. Grisenti, J. Phys. B **20**, 5817 (1987).
[61] O. Sueoka and S. Mori, J. Phys. B **22**, 963 (1989).
[62] E. Bruche, Ann. Phys. (Leipzig) **4**, 387 (1930).
[63] R. K. Jones, J. Chem. Phys. **82**, 5424 (1985).
[64] J. Ferch, B. Grantiza, and W. Raith, J. Phys. B **18**, L445 (1985).
[65] K. Floeder, D. Fromme, W. Raith, A. Schwab, and G. Sinapius, J. Phys. B **18**, 3347 (1985).
[66] O. Sueoka and S. Mori, J. Phys. B **19**, 4035 (1986).
[67] B. Lohmann and S. J. Buckman, J. Phys. B **19**, 2565 (1986).
[68] H. Nishimura and T. Sakae, Jpn. J. Appl. Phys. **29**, 1372 (1990).
[69] G. Karwasz and A. Zecca (private communication).
[70] C. Szmytkwoski and K. Maciag, Chem. Phys. Lett. **129**, 321 (1986).
[71] S. Mori, Y. Katayama, and O. Sueoka, At. Coll. Res. Jpn. **11**, 19 (1985).
[72] N. F. Mott and H. S. W. Massey, *The Theory of Atomic Collisions* (Oxford University, New York, 1965).
[73] F. A. Gianturco and D. G. Thompson, Chem. Phys. Lett. **14**, 110 (1976).
[74] F. A. Gianturco and A. Jain, Phys. Rep. **143**, 347 (1986).
[75] A. Jain and D. G. Thompson, J. Phys. B **16**, 1113 (1983).
[76] S. Hara, J. Phys. Soc. Jpn. **22**, 710 (1967); S. Salvini and D. G. Thompson, J. Phys. B **14**, 3797 (1981).
[77] J. K. O'Connel and N. F. Lane, Phys. Rev. A **27**, 1893 (1983).
[78] N. T. Padial and D. W. Norcross, Phys. Rev. A **29**, 1742 (1984).
[79] F. A. Gianturco, A. Jain, and L. C. Pantano, J. Phys. B **23**, 571 (1987).
[80] M. A. Morrison, Comput. Phys. Commun. **21**, 63 (1980); L. A. Collins, D. W. Norcross, and G. B. Schmid, *ibid.* **21**, 79 (1980).
[81] D. G. Thompson (private communication).
[82] K. L. Baluja and A. Jain (unpublished).
[83] A. D. McLean and M. Yoshmine, Int. J. Quantum. Chem. **1S**, 313 (1967).
[84] F. A. Gianturco (private communication).
[85] G. Staszewska, D. W. Schwenke, D. Thirumalai, and D. G. Truhlar, J. Phys. B **16**, L281 (1983); Phys. Rev. A **28**, 2740 (1983); G. Staszewska, D. W. Schwenka, and D. G. Truhlar, J. Chem. Phys. **81**, 335 (1984); Phys. Rev. A **29**, 3078 (1984).
[86] F. Calogero, *Variable Phase Approach to Potential Scattering* (Academic, New York, 1974).
[87] A. Jain and K. L. Baluja (unpublished).
[88] T. F. O'Mally, L. Spruch, and L. Rosenberg, J. Math. Phys. **2**, 491 (1961).
[89] M. Fink, K. Jost, and D. Hermann, Phys. Rev. A **12**, 1374 (1975).
[90] C. R. Lloyed, P. J. O. Teubner, E. Weigold, and B. R. Lewis, Phys. Rev. A **10**, 175 (1974).
[91] B. van Wingerden, W. Weigold, F. J. de Heer, and K. J. Nygaad, J. Phys. B **10**, 1345 (1977).
[92] T. W. Shyn and W. E. Sharp, Phys. Rev. A **24**, 1734 (1981).
[93] D. Rapp and P. Englander-Golden, J. Chem. Phys. **43**, 1471 (1965).
[94] R. W. Molof, T. M. Miller, H. L. Schwartz, B. Bederson, and J. T. Park, J. Chem. Phys. **61**, 1816 (1974); R. W. Molof, H. L. Schwartz, T. M. Miller, and B. Bederson, Phys. Rev. A **10**, 1131 (1974).
[95] N. T. Padial, Phys. Rev. A **32**, 1379 (1985).
[96] A. Jain and D. W. Norcross (unpublished).
[97] J. L. Dehmer, J. Siegel, J. Welch, and D. Dill, Phys. Rev. A **21**, 101 (1980).
[98] P. E. Cade and A. C. Wahl, At. Data Nucl. Data Tables **13**, 339 (1974).
[99] T. Wedde and T. G. Strand, J. Phys. B **7**, 1091 (1974).
[100] T. D. Mark and F. Egger, J. Chem. Phys. **67**, 2632 (1977).
[101] K. L. Baluja and A. Jain (unpublished).